

777 112 0097

12

AD-A231 003

**Tribological Performance and Deformation of Sputter-
Deposited MoS₂ Solid Lubricant Films During Sliding
Wear and Indentation Contact**

Prepared by

M. R. HILTON, R. BAUER, and P. D. FLEISCHAUER
Chemistry and Physics Laboratory
Laboratory Operations

DTIC
S D
JAN 16 1991

15 December 1990

Prepared for

SPACE SYSTEMS DIVISION
AIR FORCE SYSTEMS COMMAND
Los Angeles Air Force Base
P. O. Box 92960
Los Angeles, CA 90009-2960

Development Group

THE AEROSPACE CORPORATION
El Segundo, California

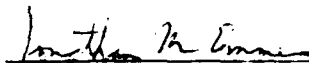
This report was submitted by The Aerospace Corporation, El Segundo, CA 90245, under Contract No. F04701-88-C-0089 with the Space Systems Division, P.O. Box 92960, Los Angeles, CA 90009-2960. It was reviewed and approved for The Aerospace Corporation by J. M. Straus, Director, Chemistry and Physics Laboratory. Lt Borden was the project officer for the Mission-Oriented Investigation and Experimentation (MOIE) Program.

This report has been reviewed by the Public Affairs Office (PAS) and is releasable to the National Technical Information Service (NTIS). At NTIS, it will be available to the general public, including foreign nationals.

This technical report has been reviewed and is approved for publication. Publication of this report does not constitute Air Force approval of the report's findings or conclusions. It is published only for the exchange and stimulation of ideas.



MARK W. BORDEN, Lt, USAF
MOIE Project Officer
SSD/MWBA



JONATHAN M. EMMES, Maj, USAF
MOIE Program Manager
AFSTC/WCO OL-AB

UNCLASSIFIED

SECURITY CLASSIFICATION OF THIS PAGE

REPORT DOCUMENTATION PAGE

1a REPORT SECURITY CLASSIFICATION Unclassified		1b RESTRICTIVE MARKINGS	
2a SECURITY CLASSIFICATION AUTHORITY		3 DISTRIBUTION/AVAILABILITY OF REPORT Approved for public release; distribution unlimited.	
2b DECLASSIFICATION/DOWNGRADING SCHEDULE			
4 PERFORMING ORGANIZATION REPORT NUMBER(S) TR-0089(4945-03)-4		5 MONITORING ORGANIZATION REPORT NUMBER(S) SSD-TR-90-52	
6a NAME OF PERFORMING ORGANIZATION The Aerospace Corporation Laboratory Operations	6b OFFICE SYMBOL (if applicable)	7a NAME OF MONITORING ORGANIZATION Space Systems Division	
6c ADDRESS (City, State, and ZIP Code) 11 Segundo, CA 90245-4691		7b ADDRESS (City, State, and ZIP Code) Los Angeles Air Force Base Los Angeles, CA 90009-2960	
8a NAME OF FUNDING/SPONSORING ORGANIZATION	8b OFFICE SYMBOL (if applicable)	9 PROCUREMENT INSTRUMENT IDENTIFICATION NUMBER F04701-88-C-0089	
8c ADDRESS (City, State, and ZIP Code)		10 SOURCE OF FUNDING NUMBERS	
		PROGRAM ELEMENT NO	PROJECT NO
		TASK NO	WORK UNIT ACCESSION NO.
11 TITLE (Include Security Classification) Tribological Performance and Deformation of Sputter-Deposited MoS ₂ Solid Lubricant Films During Sliding Wear and Indentation Contact			
12 PERSONAL AUTHOR(S) Hilton, Michael R.; Bauer, Reinhold; and Fleischauer, Paul D.			
13a TYPE OF REPORT	13b TIME COVERED FROM TO	14 DATE OF REPORT (Year, Month, Day) 1990 December 15	15 PAGE COUNT 38
16 SUPPLEMENTARY NOTATION * Solid lubricant films * Lubrication films			
17 COSATI CODES		18 SUBJECT TERMS (Continue on reverse if necessary and identify by block number)	
FIELD	GROUP	Adhesion, Solid lubricants	
		Brale indentation, Thin film deformation, Tribology	
		MoS ₂	
19 ABSTRACT (Continue on reverse if necessary and identify by block number) Microstructural aspects of the plastic deformation of sputter-deposited MoS ₂ solid lubricant films on 440C bearing steel are presented. The films were produced in three different laboratories using radio frequency, direct current, and radio frequency magnetron sources. Two types of contact were investigated: (1) sliding wear contact in a thrust-washer apparatus used to evaluate film tribological performance, and (2) brale indentation contact used to investigate cross-sectional morphology and adhesion. Scanning electron microscopy, X-ray diffraction, Auger electron spectroscopy, and x-ray photoelectron spectroscopy were used to characterize the films. The as-deposited morphology was found to influence the initial nature of the wear debris and the load-bearing capabilities of the films. In many cases, a highly deformed region confined to the surface of the films was found. Applied stress reoriented crystallites and induced crystallization. The degree of both processes was related to the initial structure and the percentage of wear lifetime of the film.			
20 DISTRIBUTION/AVAILABILITY OF ABSTRACT <input type="checkbox"/> UNCLASSIFIED/UNLIMITED <input checked="" type="checkbox"/> SAME AS RPT <input type="checkbox"/> DTIC USERS		21 ABSTRACT SECURITY CLASSIFICATION Unclassified	
22a NAME OF RESPONSIBLE INDIVIDUAL		22b TELEPHONE (Include Area Code)	22c OFFICE SYMBOL

PREFACE

The authors thank B. D. McConnell and L. L. Fahrenbacher for helpful discussions, and B. C. Stupp (Hohman Plating, Inc.) and E. W. Roberts (National Centre of Tribology, United Kingdom) for providing the DC and RFM films examined in this investigation. The assistance of P. Adams with the X-ray diffraction experiments is also acknowledged.

Accession For	
NTIS CRASH	J
DND TAB	11
Unass. ordered	11
Justification	
By	
Distribution/	
Availability Codes	
Dist	Availability or Special
A-1	



CONTENTS

PREFACE.....	1
I. INTRODUCTION.....	7
II. EXPERIMENTAL.....	11
III. RESULTS.....	13
IV. DISCUSSION.....	31
V. CONCLUSIONS.....	35
REFERENCES.....	37

FIGURES

1.	AES Sputter Profiles of Various MoS ₂ Films.....	17
2.	MoS ₂ Film Wear Lifetime in the Thrust-Washer Test as a Function of As-Deposited Thickness.....	18
3.	XRD Intensities of the MoS ₂ (002) Basal-Plane Reflection as a Function of <u>Percentage</u> Lifetime in the Thrust-Washer Test.....	19
4.	XRD Intensities of the MoS ₂ (002) Basal Plane, (100), and (110) Edge-Plane Reflections for a Film as a Function of <u>Percentage</u> Lifetime in the Thrust-Washer Test.....	21
5.	SEM Micrographs of 150-kg Rockwell "C" Indentations.....	22-23
6.	Delamination Length Plus Indentation Radius as a Function of Load.....	24-25
7.	SEM Micrographs Showing Possible Substrate Influences on Film Deformation.....	26
8.	SEM Micrographs of RFM Zone 2 Films 1 μm Thick as a Function of Presputter.....	29

TABLES

1.	Film Density.....	14
2.	XRD Data.....	14
3.	AES Results.....	16
4.	Thrust-Washer Test Results.....	16

I. INTRODUCTION

Molybdenum disulfide (MoS_2) is a useful solid lubricant because it deforms plastically more readily than the solid surfaces between which it is placed. On the macroscopic scale, the low shear strength of MoS_2 reduces the friction between sliding surfaces. On the atomic scale, the low shear strength (low friction) of MoS_2 is explained by its anisotropic crystal structure: the material is comprised of hexagonally packed planes consisting of a layer of Mo bounded on each side by a layer of S. All effective strong bonding is within the resulting "sandwich" planes, not between adjacent sandwiches. MoS_2 is strong in two dimensions and weak in the third, making the material a two-dimensional mechanical analog to one-dimensional linear polymers. The low-shear-strength basal planes provide an atomic mechanism for single-crystal plastic deformation; this mechanism plays a role similar to that of dislocations in close-packed metals. However, on the microstructural scale, which relates atomistic and macroscopic phenomena, the mechanisms of MoS_2 plastic deformation have not been fully explained. For example, MoS_2 lubricants are polycrystalline, and while the basal-plane slip mechanism explains deformation within a single crystal, the nature of the intercrystalline slip and its contribution to overall deformation are not understood at this time.

Sputtering provides a method of applying MoS_2 as a lubricant in thin-film form; it avoids the use of the organic binders used in powder applications, which can outgas in the vacuum of space. Studies have been reported that attempt to relate MoS_2 sputter-deposition conditions to film mechanical properties, such as friction and wear, and oxidation resistance (Refs. 1-5). An increasing emphasis has been placed on elucidating the physical properties of films, such as composition, crystallinity, crystal orientation, and adhesion, in order to explain the effects of deposition conditions on film performance (Refs. 6-23). Recently, we have shown (Ref. 23) that structure-zone models (Refs. 24-26) can provide a convenient conceptual framework for relating growth conditions to the physical properties of MoS_2 films.

The zone models use the dominant diffusion mechanism operating during growth as a classification criterion. The zone 1 structure is the result of a low (or absent) adatom mobility that is insufficient to overcome the effect of the shadowing favored at low T/T_m (deposition and melting temperatures, respectively) and high gas pressures. [In general, increasing gas pressure enhances the shadowing of the impinging flux, as well as decreasing the kinetic energy of ion bombardment in plasma deposition processes. Gas pressure was added by Thornton (Refs. 24,25) to the original model of film formation via evaporation developed by Movchan and Demchishin (Ref. 26) as an additional measure, along with homologous temperature, of the degree to which adatom mobility is affected by deposition conditions.] The morphology of zone 1 films consists of large dome-capped grains that have poorly defined fibrous interiors. The films can be amorphous or crystalline, they often contain voids, and they generally have poor mechanical properties. The zone 2 structure results when surface diffusion dominates; this structure consists of well-defined columnar grains that have faceted or flat tops. The zone 3 structure occurs when lattice diffusion dominates. Grain growth or recrystallization can occur, promoting large columnar grains or equiaxed grains, respectively. The mechanical properties of zone 2 and zone 3 structures are better than those of zone 1 structures. Thornton also defined a zone T (transition) morphology, favored by lower gas pressures and a higher T/T_m , that was between the zone 1 and 2 structures. The zone T material has the zone 1 fibrous interior, but with flat tops; it is not porous and its mechanical properties can be good.

In the particular case of sputter-deposited MoS_2 , we found that films from three different sources could be classified as having modified zone 1 or 2 morphologies (Ref. 23). The zone 1 films were morphologically dense [no obvious voids were present as viewed by scanning electron microscopy (SEM)], had fibrous interiors and curved tops ("cauliflower" appearance), and possessed no long-range crystallographic order as determined by X-ray diffraction (XRD). The zone 2 films were columnar and crystalline, indicating that adatom surface diffusion during film growth was occurring.

However, columnar plates were observed instead of equiaxed columns, and film porosity was present between the plates. The platelike morphology appears to be a consequence of the anisotropic crystal structure and bonding of MoS_2 , in that growth in edge directions was found to be faster than growth in basal directions. Transmission electron microscopy (TEM) studies of the early stages of zone 2 MoS_2 film growth revealed individual crystallites with both basal or edge orientations relative to the plane of the substrate surface (Ref. 27). The edge-oriented regions quickly grow and effectively shadow the basal islands, which yields voids between the evolving plates. Porosity in the zone 2 films increased with deposition temperature.

Chemical effects can also influence morphology. The zone models were developed in the context of experiments on single-element film formation. When more than one element is present, chemical interactions can affect mobility and structure. Such interactions can arise from heats of formation (Ref. 28) or the presence of impurities (Refs. 24,25). Buck has clearly shown that the presence of water during deposition inhibits mobility (Ref. 15). The addition of water vapor during deposition induced a zone 1 morphology, even at 100°C. Roberts has been able to produce RFM films that have zone 2 morphologies, by operating at higher growth rates than the rate used to synthesize the RFM films reported here (Ref. 17). He suggests that increasing the MoS_2 deposition flux while maintaining a fixed water-vapor flux decreases the relative immobilizing effect of the water. The presence of oxygen will be discussed further in Sections 3 and 4.

In our previous study, examination of films deposited by three different sources before and after sliding wear showed that when the lubrication ability of sputter-deposited MoS_2 films is assessed, both the as-deposited and deformed microstructures, including crystalline orientation and morphology, must be considered (Ref. 23). In particular, we showed that deformation at low loads can be confined to a surface region in some morphologically dense zone 1 and zone 2 microstructures. In the zone 1 films, XRD and cross-sectional SEM showed that stress-induced crystallization had occurred in the surface deformed zone, yielding basal-

plane orientation parallel to the substrate. As will be shown in Sections 3 and 4, this crystallization apparently provides sufficient lubrication to yield good wear life. When sliding-wear tests are performed on the zone 2 films, a crystal reorientation occurs in which some of the basal planes are realigned parallel to the substrate (Refs. 20, 21, 23). Aspects of this process will be discussed in this report.

Our previous study (Ref. 23) focused on the structural changes that occur during sliding wear. To provide a more comprehensive view of the relationship between film physical properties and tribological performance, in this report, we present complementary information, including the density, composition, and crystallinity of MoS₂ films, film wear-life data, and aspects of film adhesion during indentation contact.

11. EXPERIMENTAL

The MoS_2 films on 440C bearing steel were studied in three different laboratories, each of which prepared the films by a different sputtering technique: (1) radio frequency sputtering (Ref. 21), (2) direct current sputtering (Refs. 3,5), and (3) radio frequency magnetron sputtering (Refs. 17-18). For convenience, these films will be referred to as RF, DC, and RFM, respectively. Typical deposition temperatures, pressures, and growth rates were as follows: RF: 70-220°C, 2.66 Pa, 245-345 Å/min; DC: 130-175°C, 3.06 Pa, 600 Å/min; RFM: 25-70°C, 2.66 Pa, 400-600 Å/min. Some of the DC films contained codeposited nickel (Refs. 3,5). It is worth emphasizing that the RF and DC films were formed in contact with the plasma during growth, while the RFM films were deposited when the plasma was magnetically confined away from the surface of the film. Surface adatom mobility, which is influenced by substrate temperature (which in turn is affected by secondary-electron bombardment), should be lower in the RFM case. The substrates were sputter-precleaned in the DC and RFM experiments, but not in the RF experiments. Previous scanning electron microscopy (SEM) and X-ray diffraction (XRD) experiments have shown that the RF and DC films reported here have a columnar-plate zone 2 morphology, with the (100) and (110) edge plane being the preferred orientation parallel to the substrate. The RFM films had two different morphologies: A fibrous zone 1 morphology, with little or (often) no crystallinity detected by XRD; or a zone 2 morphology. The cause for the difference in morphology will be discussed in the next section.

The sliding-wear deformation was produced by a thrust-washer apparatus under conditions described previously (Ref. 21). Briefly, the machine consists of a disk that slides against a coated flat under low loads (3.18 kg dead weight) at a mean sliding velocity of 33 mm/s. The apparent contact area between the rider and the stationary member was approximately 45.2 mm². In some tests, films were run until they failed (arbitrarily defined as that point where the reaction torque of the stationary member

exceeded 0.07 Nm). Other tests were terminated after a fixed number of revolutions; then, XRD characterization measurements were made. In some cases, testing was resumed after XRD analysis. Thickness and density measurements were made by passing a stylus across steps in the films and by weighing. SEM observations of the stylus tracks were performed to account for the effect of film deformation, which could reduce the thickness of the step relative to that of the original film, as reported earlier (Ref. 21). X-ray photoelectron spectroscopy (XPS) and Auger electron spectroscopy (AES) were used to ascertain film composition; these procedures are detailed elsewhere (Ref. 21).

The films were indented with a Rockwell "C" diamond braze stylus. The radial compressive load generated at the indentation rim caused the film to fracture, reproducibly exposing cross sections. These cross sections were the initial objects of interest (Ref. 29). However, it was quickly observed that the nature and extent of film delamination varied for different samples, and that this variation might provide a means of assessing interfacial fracture toughness. Indentations were then made at various loads that ranged in discrete steps from 15 to 150 kg. Crack growth as a function of load was measured later by SEM, following the approach used by Jindal et al. (Ref. 30), who have investigated hard coatings such as TiN, TiC, and Al₂O₃ to assess interfacial fracture toughness, which is affected by film-substrate adhesion.

III. RESULTS

Film densities are listed in Table 1. The results vary widely. Furthermore, the zone 2 films (RF and DC) are heterogeneous structures of voids and platelets, and the average densities are not the density of the material inside the platelets. The results of XRD on film orientation are listed in Table 2; the preferred orientation is often seen. The films appear similar, except for the RFM zone 1 "A" films, in which no peaks were detected by XRD. When film thickness and density are considered, it appears that the RF high temperature (HT) films are the most crystalline, the RF ambient temperature (AT) and DC films are moderately crystalline, and the RFM zone 1 films are the least crystalline. This crystallinity ranking is consistent with the film morphologies, in that the least crystalline films (RFM) have the zone 1 morphology, which results from an inhibited adatom mobility during deposition that would also inhibit epitaxial growth.

Compositional analysis indicates that the RFM zone 1 films contain more oxygen than the RF or DC films. XPS of the RF films combined with sample heating in ultrahigh vacuum have shown that the oxygen exists in at least two forms: (1) as an $\text{MoS}_{2-x}\text{O}_x$ phase (with 5 to 15% oxygen within that phase in the RF films) and (2) as MoO_3 (Ref. 31). The RF films contain between 90 and 99% of the $\text{MoS}_{2-x}\text{O}_x$ phase, and the DC films contain more than 98% of the $\text{MoS}_{2-x}\text{O}_x$ phase. The RFM zone 1 films contained between 60 and 80% of the $\text{MoS}_{2-x}\text{O}_x$ phase (Mo^{4+}), with the balance being other oxides (MoO_3), while the RFM zone 2 films have 80-85% of the $\text{MoS}_{2-x}\text{O}_x$ phase. Buck has shown that the presence of water vapor during MoS_2 sputter deposition can yield films with the zone 1 morphology and a high oxygen content (Ref. 15). The RFM zone 1 films appear to be the result of oxygen that originates from a new deposition system, as recently produced RFM films have a zone 2 morphology. AES analysis (Table 3) agrees with the XPS data. The low energy ratios indicate that the RFM zone 1 "B" films are sulfur deficient at the immediate surface, whereas the DC films are sulfur

Table 1. Film Density

ID	Density
RFM Zone 1 A	1.61 ± 0.08
RFM Zone 1 B	4.07 ± 0.48
RFM Zone 2	1.80 ± 0.18
DC Zone 2	0.77 ± 0.07
DC Zone 2 Ni	0.93 ± 0.09
RF Zone 2 AT	3.03 ± 0.42
RF Zone 2 HT	2.05 ± 0.20

MoS₂ Crystal 4.8

Table 2. XRD Data

ID	(100)/(110) Ratio	Peak Location (2θ, deg)	
		(100)	(110)
RFM Zone 1 A	ND ^a	ND	ND
RFM Zone 1 B	2.58	34.6	61.6
RFM Zone 2	5.17	34.2	60.0
DC Zone 2	2.67, 3.05	33.6	59.9
DC Zone 2 Ni	2.80	33.6	59.6
RF Zone 2 AT	2.70-3.60	~33.7	~60.2
RF Zone 2 HT	3.70-5.20	~33.7	~60.0

^aNo edge-plane reflections were detected.

rich. The ratio at higher energy, i.e., at deeper sample depth, shows that all films are sulfur deficient below the surface. AES sputter depth profiling (Fig. 1) yielded generally constant compositions during film removal, except for a sulfur accumulation observed in some of the RFM zone 1 "B" films. [Apparently, these were made before the other films were deposited (e.g., RFM zone 1 "A"), which supports the idea that the deposition system was initially unstable.]

The results of the thrust-bearing wear test are listed in Table 4. The films show a similar dependence of wear life with thickness (Fig. 2): below a critical thickness, effective lubrication does not occur, while above some optimum thickness, additional gains of wear life with increased thickness are small. Spalvins observed this critical thickness phenomenon, although he did not find any gains in wear life above the optimum thickness (Ref. 10.) In his pin-on-disk wear test (Ref. 6), wear debris was quickly removed from the wear track, while in our test, debris is probably retained for longer periods.

As reported in a previous study (Ref. 23), when sliding wear tests are performed on zone 2 films, a crystal reorientation occurs in which some of the basal planes are realigned parallel to the substrate, thus facilitating lubrication. The zone 1 films, which as deposited have little or no crystallinity, undergo a stress-induced crystallization at the surface, which yields a basal-plane orientation in the wear track. Previous SEM and XRD studies showed that the zone 2 reorientation occurred very quickly as a function of absolute wear life for films deposited at higher temperature. These films had a lower platelet-packing density and fractured and deformed more easily than films deposited at ambient temperature. More recent analysis has focused on basal-plane reorientation/crystallization as a function of the percentage of wear life. Figure 3 shows that the zone 2 films reorient early in wear life, and then the signal that indicates basal-plane orientation decreases, presumably because film material is ejected from the wear track. Basal-plane crystallization occurs more slowly for the zone 1 films.

Table 3. AES Results

ID	(S/Mo) _L ^a	(S/Mo) _H ^b	(O/Mo) _L ^c
RFM Zone 1 A	8.51	1.16	1.74
	8.95	1.11	1.31
RFM Zone 1 B	6.85	0.99	1.71
	7.78	1.29	1.20
DC Zone 2	9.59	0.98	0.86
	9.05	1.25	0.85
	9.75	1.32	0.56
DC Zone 2 Ni	9.66	1.40	1.71
	8.40	1.16	1.02
RF Zone 2 AT	8.99	1.40	0.88
RF Zone 2 HT	8.19	1.28	1.00
MoS ₂ Crystal	8.55	1.49	-

^aS(151 eV)/Mo(186 eV)^bS(2117 eV)/Mo(2044 eV)^cO(520 eV)/Mo(186 eV)

Table 4. Thrust-Washer Test Results

ID	Thickness, nm	Lifetime, ^a 10 ³ rev
RFM Zone 1 A	560	366
	900	305
RFM Zone 1 B	1560	849
	1560	506
RFM Zone 2	1340	611
	1340	763
DC Zone 2	1270	320
	2170	220
DC Zone 2 Ni	1060	130
	1280	230
RF Zone 2 AT	1260	1190
	1240	1180
RF Zone 2 HT	1080	390
	1080	590

^aRevolutions to failure

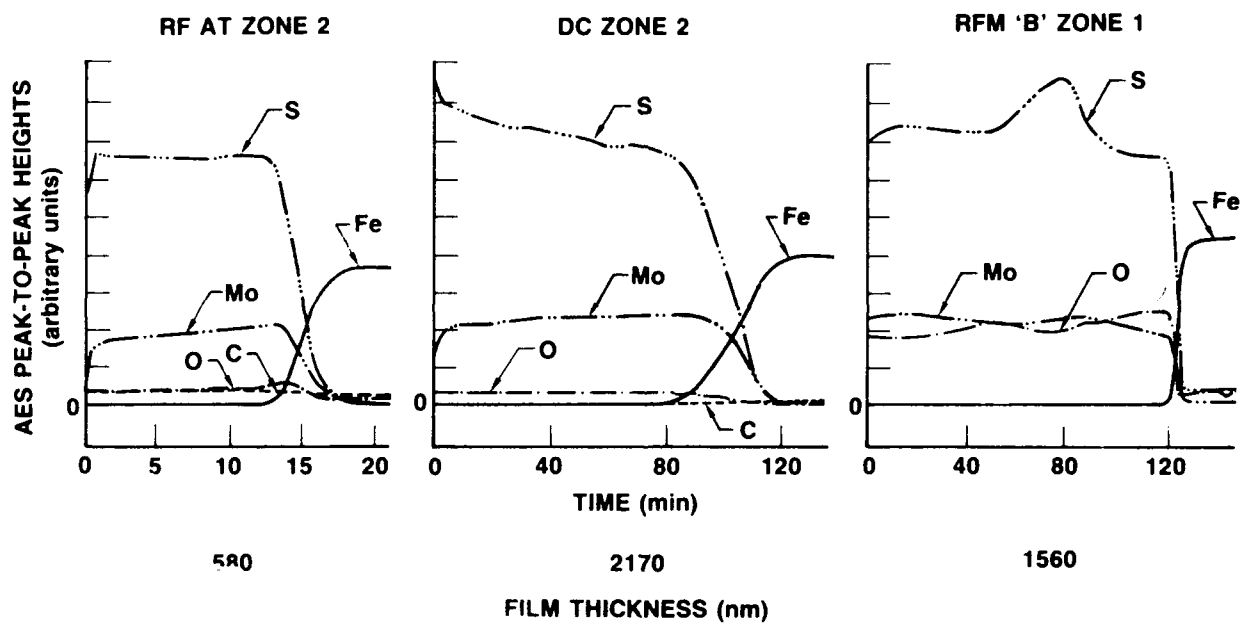


Fig. 1. AES Sputter Profiles of Various MoS₂ Films. The RFM zone 1 films contain more oxygen than the zone 2 films.

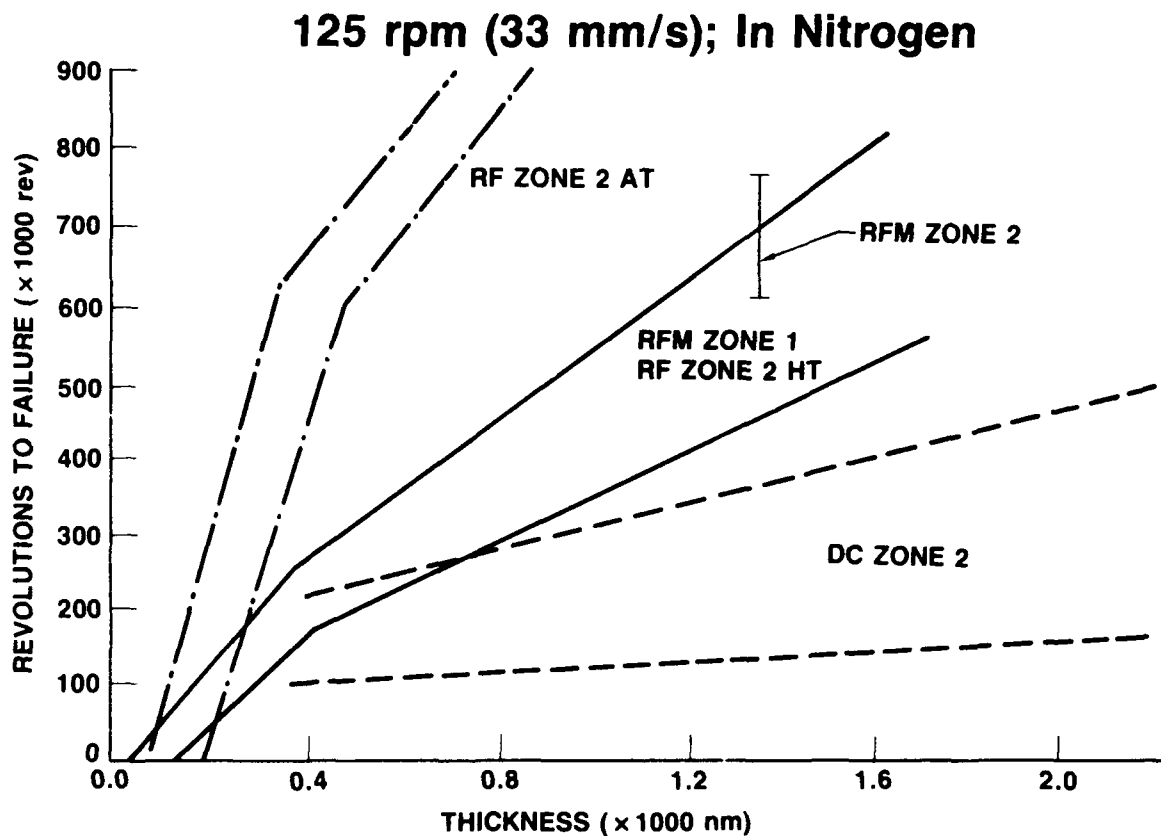


Fig. 2. MoS₂ Film Wear Lifetime in the Thrust-Washer Test as a Function of As-Deposited Thickness. Below a critical thickness, lubrication is not effective. Above an optimum thickness, increases in film lifetime with thickness are lower.

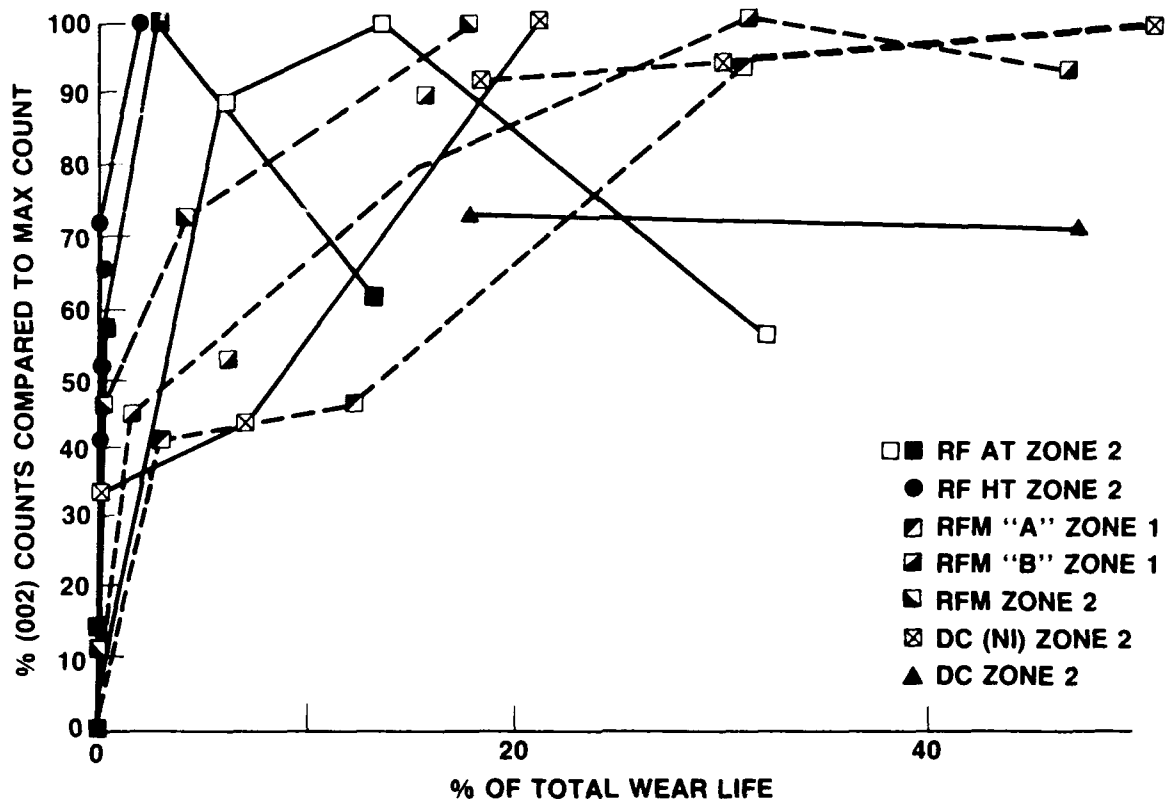


Fig. 3. XRD Intensities of the MoS_2 (002) Basal-Plane Reflection as a Function of Percentage Lifetime in the Thrust-Washer Test. Basal-plane reorientation parallel to the substrate, which enhances lubrication, occurs quickly in the zone 2 films. The initial rise is due to large-scale platelet reorientation. Subsequent decreases represent film wear. Stress-induced crystallization occurs in the zone 1 films and is confined to the film surface, which yields a slower rise in (002) intensity.

When zone 2 crystal reorientation is viewed as a function of the percentage of wear life, it appears that these films wear in a similar way (regardless of the absolute total wear life). Figure 4 shows XRD basal-plane and edge-plane reflections as a function of the percentage of wear life for an RF AT film. The initial rise of basal-plane and the fall of edge-plane reflections represent platelet reorientation at the film surface or through most of the film. Edge-plane intensities remain relatively constant for the remainder of film life, apparently because they represent underlying platelets securely bound to the interface. The drop in basal-plane intensity throughout most of film life represents the wearing away of this material that apparently is the lubricant. When this material is eliminated, failure occurs. The measured edge-plane intensities between 20 and 80% of wear life, in Fig. 4, appear equivalent to the intensities observed for as-deposited films that have the minimum thickness for effective lubrication (Fig. 2).

The qualitative nature and quantitative extent of film fracture caused by brale indentation was found to be influenced by film thickness and morphology. At high-load indentations, lateral fracture occurred and resulted in film delamination (Fig. 5A,B). The extent of delamination increased with film thickness (Fig. 6A). In addition, beyond the region of initial delamination, circumferential cracks or multiple buckling was observed in 0.5- μm RF films (Fig. 5C), while radial cracks were observed in thicker RF films (Fig. 5D). Examination of the delaminated region with SEM and energy dispersive spectroscopy (EDS) indicates that fracture occurs within the film, very close to the interface. The exposed steel surface appears to have tiny regions of elevation, which are presumably the result of deformation during indentation (Fig. 7A). In addition, chromium carbides, which are harder and more brittle than the steel matrix, develop radial fractures (Fig. 7B-D). Both the vertical matrix deformation and the carbide fracture may induce or contribute to the buckling and the radial fracture observed in the extended regions of thinner and thicker zone 2 films, respectively.

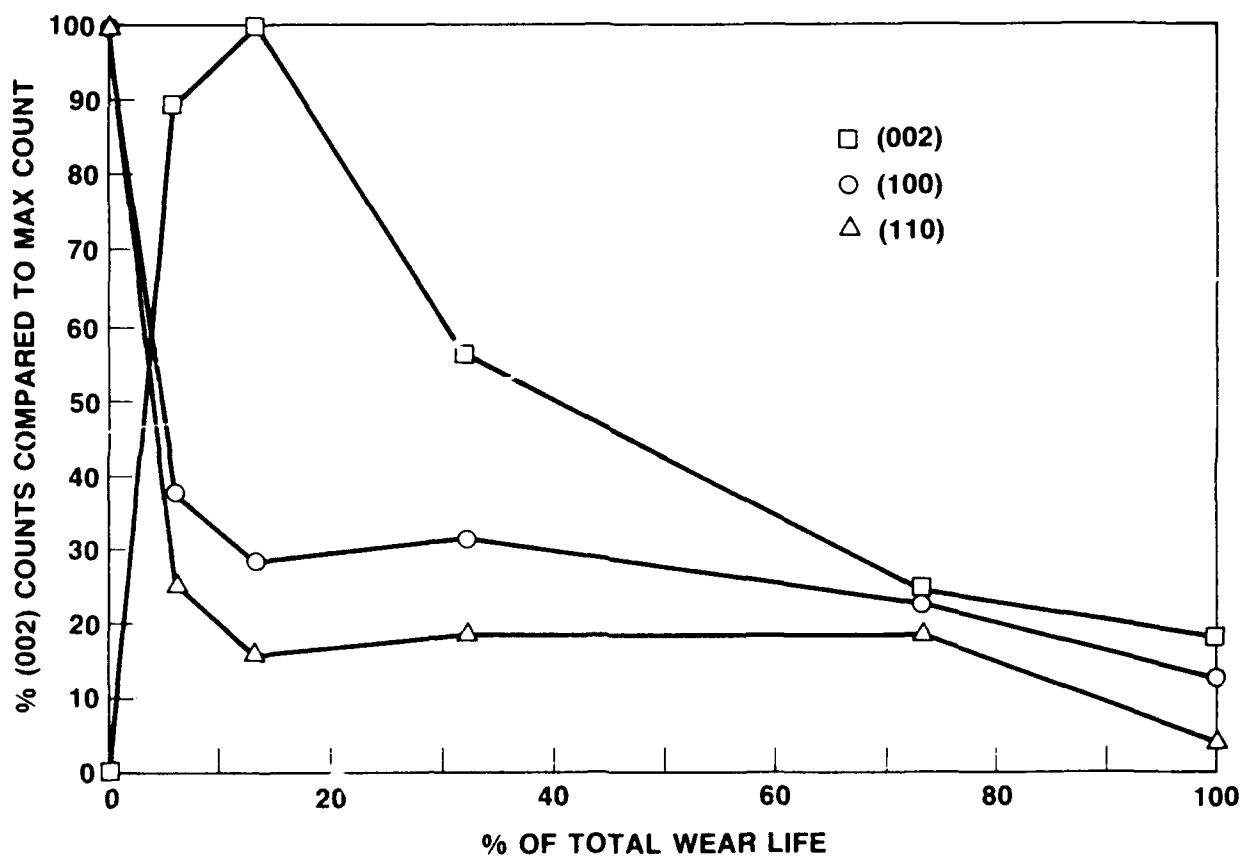


Fig. 4. XRD Intensities of the MoS_2 (002) Basal Plane, (100), and (110) Edge-Plane Reflections for a Film as a Function of Percentage Lifetime in the Thrust-Washer Test. Basal plane reorientation is similar to that in Fig. 3. The corresponding decrease in edge-plane intensity is a consequence of large-scale platelet reorientation. Throughout the majority of wear life, some edge-plane material (presumably strongly bound to the substrate) remains until failure.

Rockwell C Impact Delamination of MoS₂

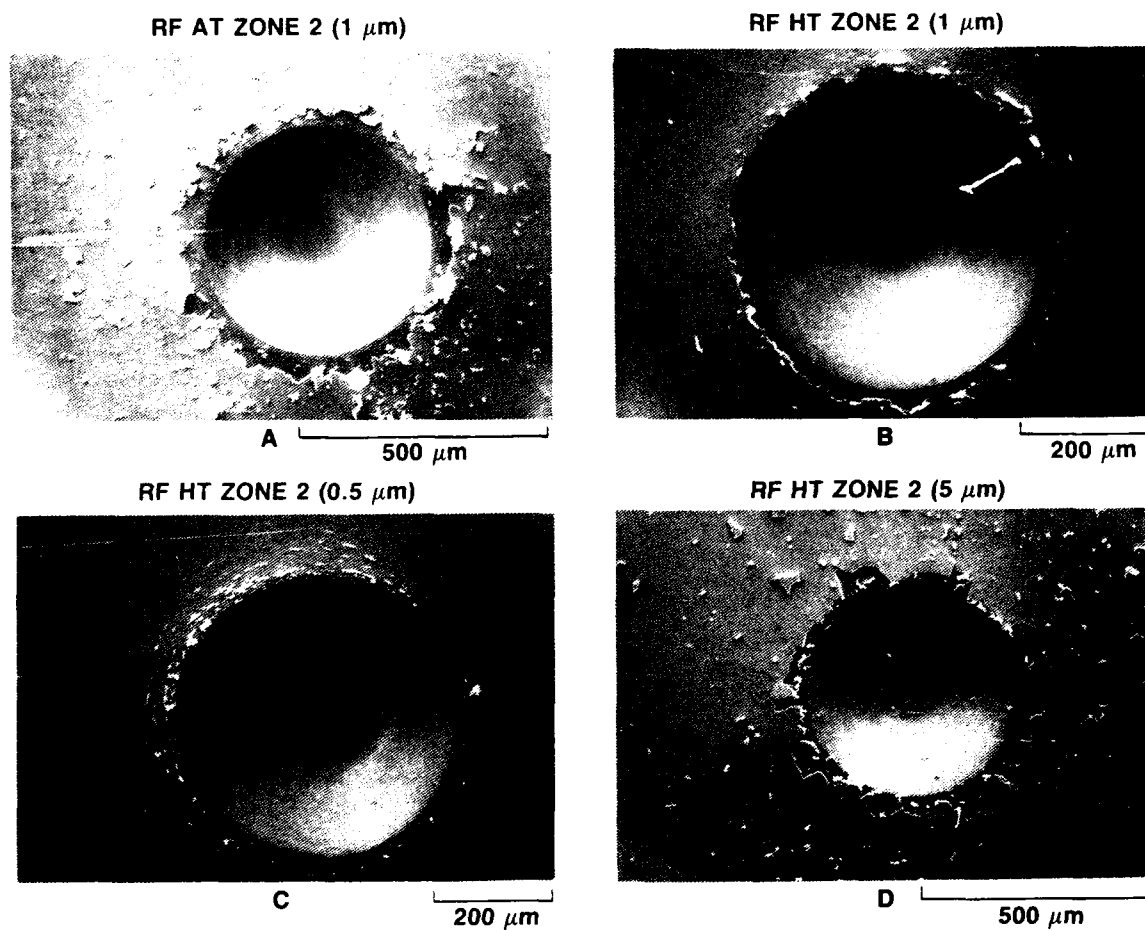
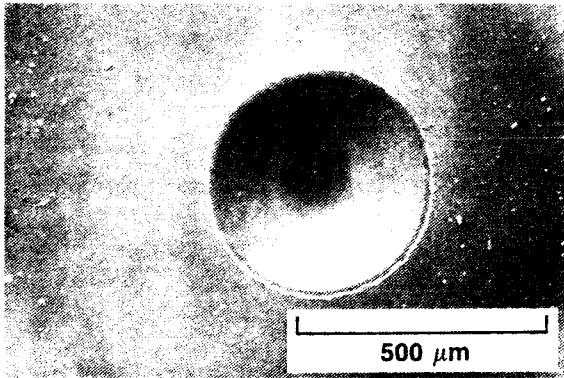


Fig. 5. SEM Micrographs of 150-kg Rockwell "C" Indentations. (A) RF AT, 1 μm , Zone 2; (B) RF HT, 1 μm , Zone 2; (C) RF HT, 0.5 μm , Zone 2; (D) RF HT, 5 μm , Zone 2.

Rockwell C Impact Delamination of MoS₂

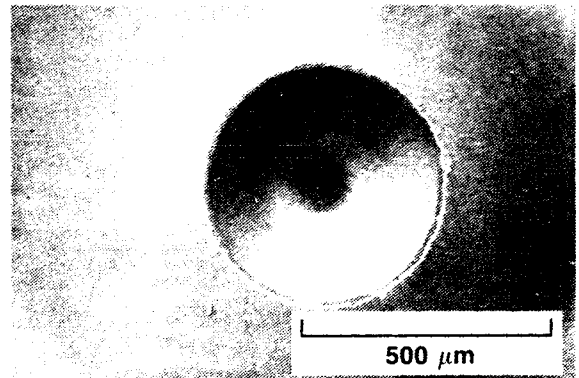
DC SPUTTERED

WITH Ni (P) (0.9 μm)



E

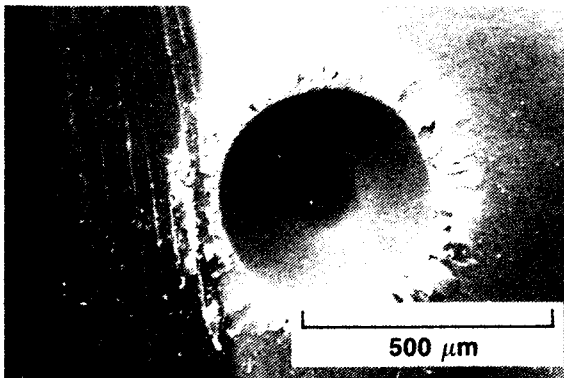
WITHOUT Ni (P) (0.9 μm)



F

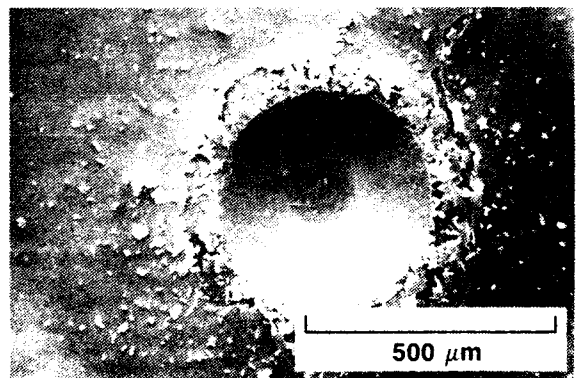
RF MAGNETRON SPUTTERED

'A' (0.8 μm)



G

B (1.5 μm)



H

Fig. 5. SEM Micrographs of 150-kg Rockwell "C" Indentations. (E) RF DC (Ni), 0.9 μm , Zone 2; (F) DC, 0.9 μm , Zone 2; (G) RFM "A", 0.8 μm , Zone 1; (H) RFM "B", 1.5 μm , Zone 1.

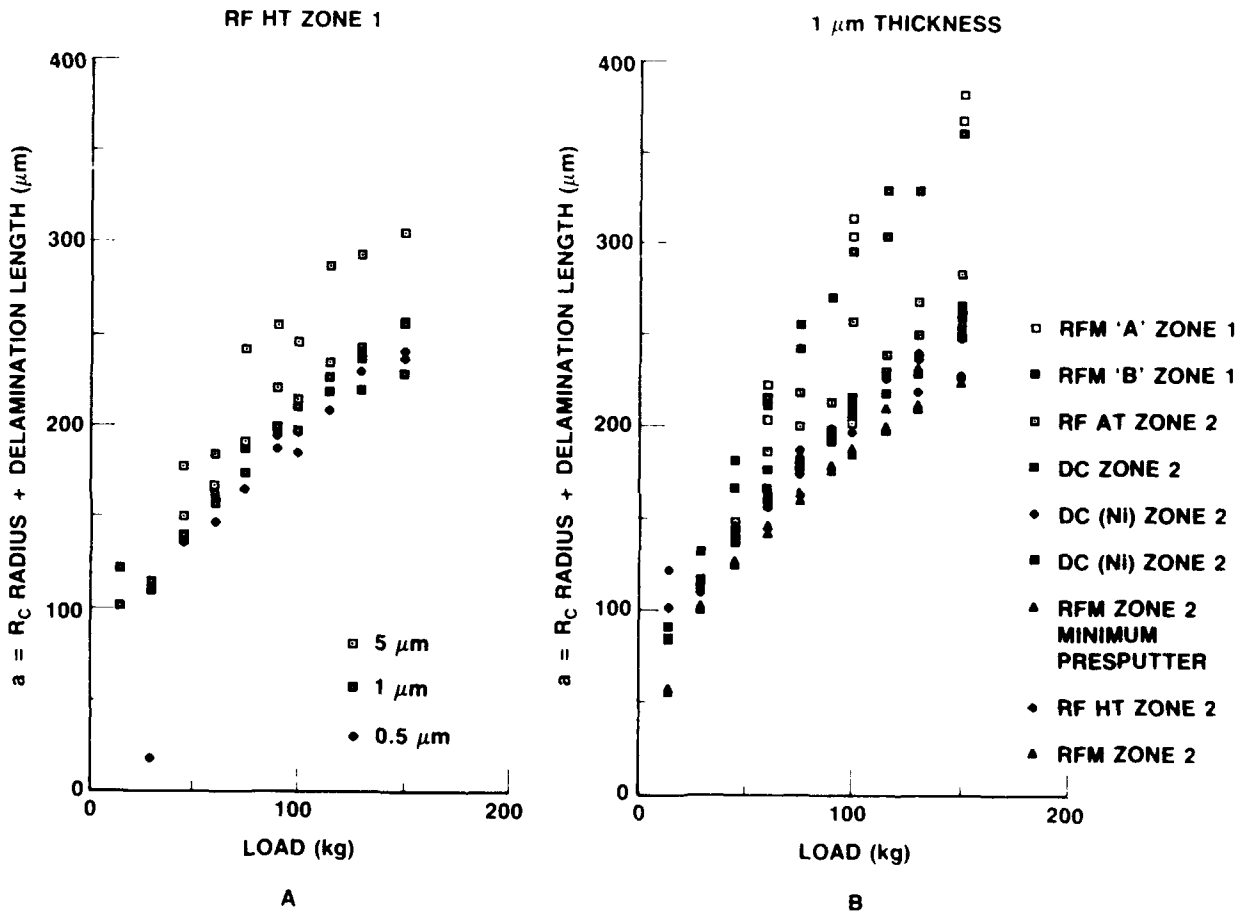


Fig. 6. Delamination Length Plus Indentation Radius as a Function of Load. (A) RF HT zone 2 films at variable thickness. (B) Various zone 1 and zone 2 films of 1 μm thickness showing a lower toughness in the zone 1 films.

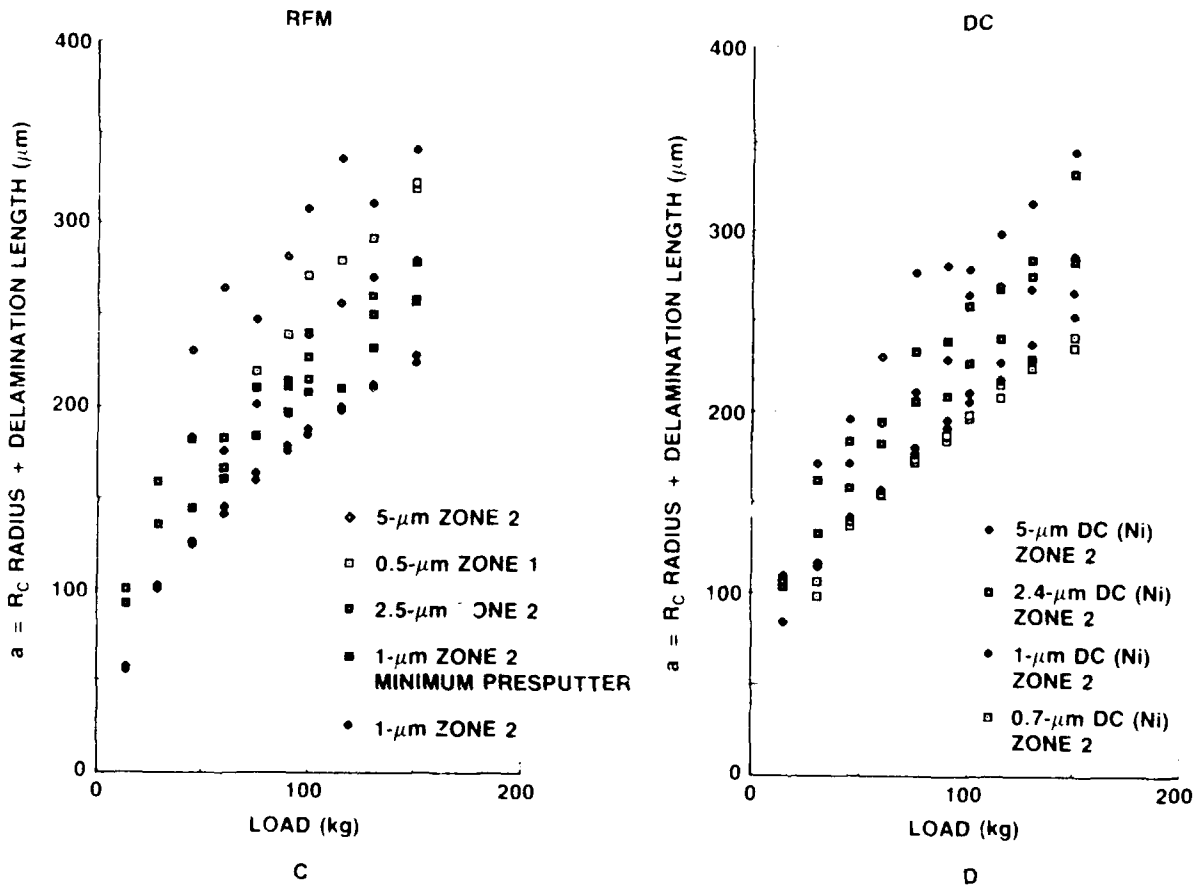


Fig. 6. Delamination Length Plus Indentation Radius as a Function of Load. (C) RFM films showing the effects of thickness, morphology, and minimum sputter pretreatment. (Unless otherwise stated, films received substrate bombardment prior to deposition.) (D) DC (Ni) zone 2 films showing the effect of thickness.

Substrate Effects on R_C Delamination

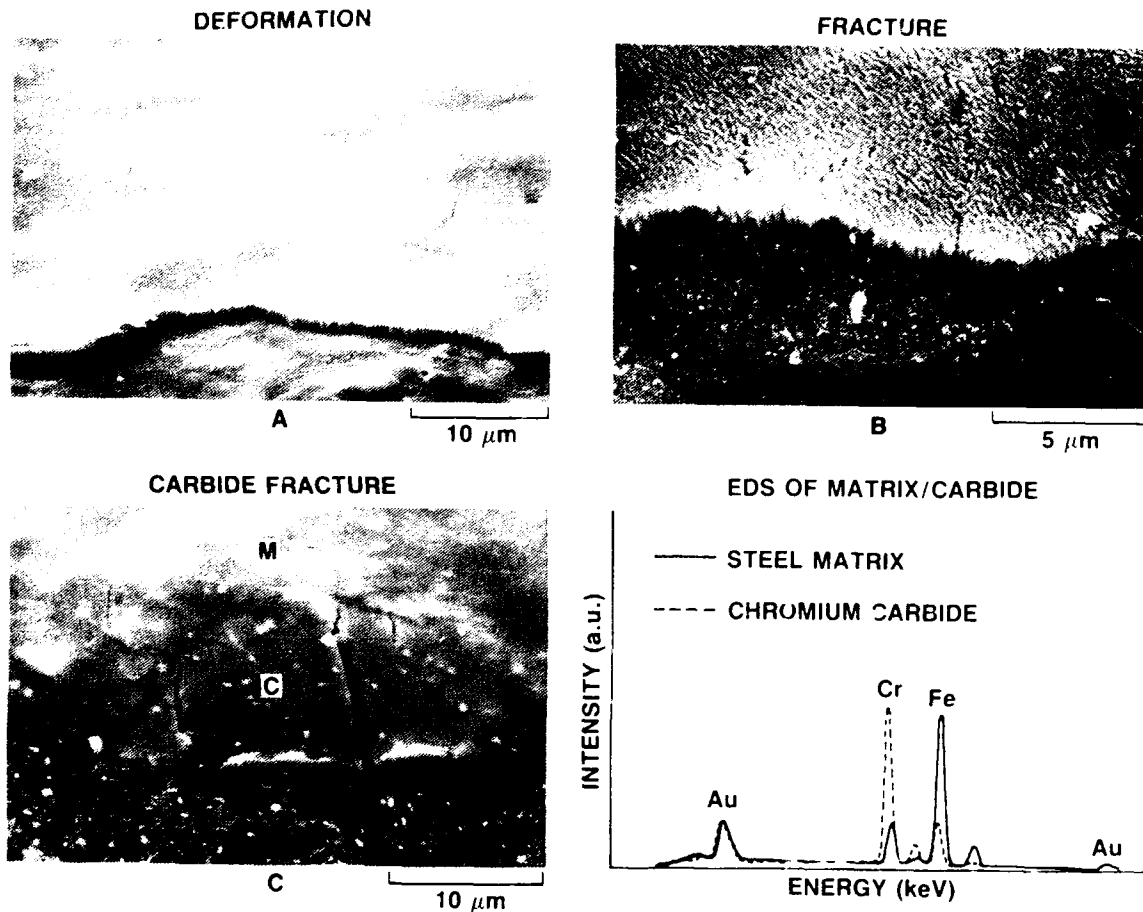


Fig. 7. SEM Micrographs Showing Possible Substrate Influences on Film Deformation. (A) Localized vertical plastic deformation of substrate and film. (B) Radial fracture in substrate and film (presumably initiated in a subsurface carbide). (C) Radial fracture in a carbide ("C") surrounded by a more ductile matrix ("M"). (D) X-ray energy dispersive spectra of the chromium carbide and steel matrix in (C).

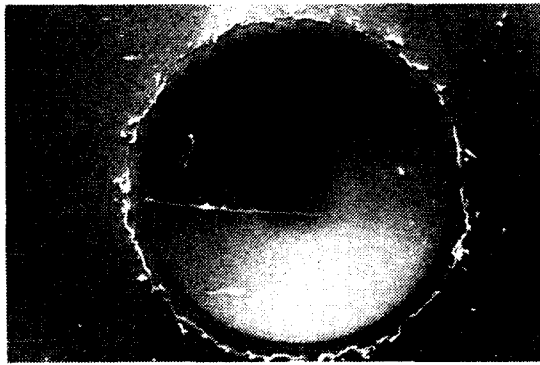
Since the length of the delaminated region varies with film thickness for a given deposition condition, films deposited under different conditions must be of identical thickness if one is to compare delamination lengths in order to evaluate fracture toughness. Figure 6B shows both the delamination length and the indentation radius, a , for films with a nominal thickness of $1 \mu\text{m}$. The RFM zone 1 films have a lower fracture toughness, K (which is inversely related to the slope da/dL), than do the zone 2 films (Fig. 5G,H). The zone 2 RF and DC films appear similar (Fig. 5A,B,E,F). This effect of morphology is highlighted by studies of recently prepared RFM films that show delamination as a function of thickness (Fig. 6C). Delamination increased with thickness except for the thinnest film, which was prepared first and had a zone 1 morphology, while the others had a zone 2 morphology. The extent of delamination of this $0.5 \mu\text{m}$ zone 1 film exceeded that of the 2.5 and $1 \mu\text{m}$ zone 2 films. Delamination also increases with film thickness in Ni-bearing zone 2 DC films (Fig. 6D). DC zone 2 film delamination was not observed to vary, due to the presence of nickel. The RF HT films have slightly shorter delamination lengths than the RF AT films.

Another value that could be determined is the minimum or critical load for the onset of fracture, P_{CR} . We have found that for most films, P_{CR} is very low, often less than 30 kg and occasionally lower than 15 kg . In addition, the delamination around the rim is often very uneven at these low loads. [Variability in delamination length is also observed in thick ($5 \mu\text{m}$) films under high loads.] Thus, we have found P_{CR} to be a less discriminating value for these soft films than K and the qualitative nature and quantitative extent of fracture. Jindal et al. have also concluded that K is more discriminating than P_{CR} for characterizing hard coatings (Ref. 30).

Substrate precleaning appears to affect K and P_{CR} . The substrates in the DC and RFM systems were generally sputter bombarded before deposition, although the RF system does not have this capability. The RFM zone 1 films initially received had a low fracture toughness because of their morphology and high oxygen content. Recently received RFM films have a zone 2

morphology, and two of these films that were 1 μm thick were prepared. One film received a minimal sputter precleaning, and delamination was evident in this film after indentation (Fig. 8A,B). However, the other film, which also received sputter precleaning, did not delaminate (Fig. 8C); rather, an abrupt fracture and folding of the film is observed at the rim (Fig. 8D). The effect of substrate precleaning on K and P_{CR} needs to be investigated further. It is clear, however, that the indentation technique can reveal differences in film response.

NO PRESPUTTERING

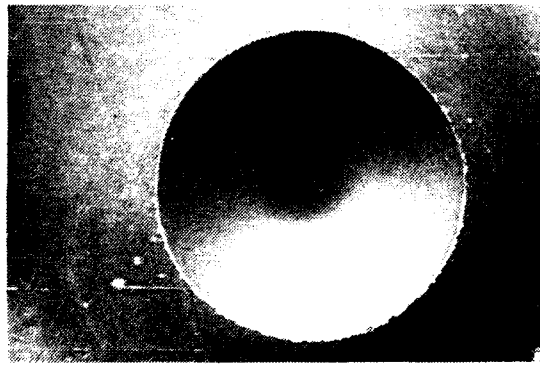


A 200 μm



B 20 μm

PRESPUTTERING



C 200 μm



D 10 μm

Fig. 8. SEM Micrographs of RFM zone 2 Films 1 μm Thick as a Function of Presputter. (A,B) Minimum substrate presputter where delamination is evident. (C,D) Normal pretreatment in which delamination is retarded. See delamination vs load data in Fig. 6C.

IV. DISCUSSION

A model of film deformation and wear can be developed from the data presented in this report as well as from earlier structural studies (Ref. 23). For the zone 2 films, the highest absolute wear life is obtained with films having the highest platelet-packing density (dense morphology) and film crystallinity ($\text{MoS}_{2-x}\text{O}_x$ phase). Lubrication is provided by platelets that are reoriented early in a film's wear life (<20% of wear life).

The degree and depth of film deformation can vary with load. Under high loads, significant amounts of the zone 2 platelets are reoriented, although some material is not reoriented. The latter presumably consists of platelets at the interface that are strongly bound to the substrate. As sliding wear continues, the reoriented material is ejected. This ejection occurs quickly below 40% of wear lifetime and more slowly beyond this value. Film failure occurs when a significant amount of the reoriented material is removed. Note that effective lubrication is provided by a small amount of reoriented zone 2 material, presumably at the surface. In the zone 1 films, stress-induced crystallization occurs at the wear surface, providing basal-plane material for lubrication. The slow formation of the basal material is a result of the crystallization process. High frictional stresses at the surface induce crystallization there. Once basal material is formed, lubrication occurs and reduces frictional stresses at the surface; this eliminates the force that causes basal-plane crystallization to occur deeper in the film. When the transformed surface material is eventually worn away, the frictional stresses rise and induce further crystallization.

The composition of the zone 1 films provides insight into the origin of the morphology and the causes of the variability of wear rates within this morphology. The zone 1 films contain significantly more oxygen than the zone 2 films. The oxygen presumably comes from oxygen or water vapor in the new deposition system that was used to make the initial films. The

presence of oxygen or water vapor can inhibit adatom mobility in the sputter deposition of MoS_2 (Ref. 15) and other materials (Ref. 24), which will cause the zone 1 morphology to evolve. We believe that the presence of oxygen in the MoS_2 films can enhance or retard lubricity. If the oxygen is in an $\text{MoS}_{2-x}\text{O}_x$ phase, lubrication is still possible (and may even be improved), while it is inhibited if the oxygen is in another phase, e.g., MoO_3 (Refs. 32,33). The zone 2 films consist of over 80% (often over 90%) of the $\text{MoS}_{2-x}\text{O}_x$ phase (with 5 to 15% oxygen within that phase in the RF films), while the zone 1 films had only 60-80% $\text{MoS}_{2-x}\text{O}_x$. The major difference detected between various zone 1 films that had good wear rates (RFM Zone 1 "A") and those that had poorer wear rates (RFM Zone 1 "B") was that the latter had less sulfur in their surface. Chronologically, the RFM Zone 1 "B" samples were made before the "A" samples. A reasonable conclusion would be that the new deposition system yielded the most oxidized, and hence the least sulfur-containing, films in the earliest deposition runs. As the system improved, film structure changed from a highly oxidized and sulfur-deficient zone 1 microstructure (a poor lubricant), to an oxidized but sulfur-sufficient zone 1 microstructure (a good lubricant), to a least-oxidized zone 2 microstructure. (Initial wear-test results indicate that the absolute wear lives of RFM Zone 2 films are similar to those of the other zone 2 films.)

The relative wear performance of the films varies with different wear tests and test conditions. Roberts has found that the RFM zone 1 films ("A" series) perform optimally in pin-on-disk tests conducted in vacuum.* Stupp has found that the DC films cosputtered with Ni perform better than the others in an A-6 dual rub-block tester in ambient air (Refs. 3,5). The tests differ in the atmosphere in which they were run (the thrust-washer test used by the authors was run in dry N_2 at atmospheric pressure), and in the nature and degree of film-debris retention in each case. Of the three tests, the pin-on-disk test [which was also used in the studies by Spalvins

* E. W. Roberts, personal communication, National Centre of Tribology, UKAEA Risley Laboratory, United Kingdom.

(Ref. 6)] probably ejects debris most readily. The A-6 tester also ejects debris, while the thrust-washer apparatus probably retains film debris the longest. Thus, in the pin-on-disk test, the dense zone 1 morphology could excel because it resists large-scale reorientation and hence the detachment of material better than the zone 2 morphology. Morphological packing density would be a determining factor, along with the adhesion of the remnant deformed layer. In the thrust-washer test, detachment is acceptable because the reoriented material is retained longer and still lubricates. The determining factor here is film density (both in the morphology of platelet-packing density and in the material density within the platelets), which determines the amount of material, per unit of deposited thickness, that is ultimately available for lubrication. The RF AT films in the present study happen to have the highest density of the $\text{MoS}_{2-x}\text{O}_x$ phase; they have the highest normalized wear-resistance rate for the thrust-washer test. The role that Ni plays in optimizing A-6 wear-test performance is not clear at this time.

For all of these tests, the microstructures of the films in the later stages of wear are worth further investigation, so that one can more accurately determine the deformed structure that provides tribological protection during the majority of film lifetime. In a previous study (Ref. 23), the nonuniform loading in the thrust-washer test made it difficult to make a quantitative SEM investigation of deformation microstructure vs wear life, particularly with respect to determining the thickness of the deformation layer as a function of the percentage of wear life. A cross-sectional SEM study of wear in the pin-on-disk test would be an improvement, because the point-contact loading in this case is more predictable. Both the structure of the remnant deformed layer and this layer's ability to adhere to the substrate will help explain how lubrication is accomplished in debris-ejecting sliding-wear contact.

The variable-load brale-indentation method does detect differences in fracture toughness among films, although the relationship between measured fracture toughness, physical properties such as interface composition, and wear properties (including effective film adhesion during sliding contact)

needs to be determined. The data show that (1) soft MoS₂ films fracture and delaminate in a manner qualitatively similar to the behavior observed in previous studies of hard coatings (Refs. 30, 34-36), (2) increasing film thickness enhances delamination, and (3) MoS₂ zone 1 morphologies delaminate more than zone 2 morphologies (for a given thickness).

Fracture-mechanics modeling based on the indentation testing of hard coatings has to date assumed that behavior is only brittle (Refs. 37-39); on the other hand, MoS₂ can readily deform plastically. However, MoS₂ is an anisotropic planar material; it is strong in two dimensions and weak in the third. In the as-deposited zone 2 material, the low-shear basal planes are perpendicular to the substrate. When indentation occurs, strong radial compressive and tangential tensile stresses parallel to the substrate are generated. There are few low-shear planes along the stress directions; rather, the stresses must displace the strongly bound atoms within the MoS₂ sandwich planes. Localized shear can occur parallel to the substrate in platelets that happen to be oriented so that their major axis is along the stress directions. Vertical shear could occur if appropriate stresses developed in any of the platelets, since the platelets are oriented perpendicular to the substrate. The mechanical modeling of this process will have to take these elements of vertical plasticity into account. The thickness effect has been experimentally observed before (Refs. 28, 34-36) and has been compensated for in modeling (Refs. 37-39). This effect is often attributed to residual stresses that add a further driving force to cause fracture. (These stresses increase with film thickness.) The lower fracture toughness of the zone 1 material may be due to (1) the lower crystallinity of the material, which would lower the basal-plane element of plasticity; or (2) the higher oxygen content of the material, which might increase brittleness; or (3) both.

V. CONCLUSIONS

In a thorough assessment of the lubrication ability of sputter-deposited MoS_2 , one must consider both the nature of film debris formation and film debris retention in the sliding-wear contact region. If sliding-wear debris is generally retained within the contact region, such as in a telescoping mechanism, film density and the ability to provide crystalline $\text{MoS}_{2-x}\text{O}_x$ of the proper orientation (as a result of either stress-induced reorientation or crystallization) are the important film properties that determine component lifetime. The thrust-washer test appears to be a reasonable discriminator when debris is retained. If, on the other hand, wear debris is quickly ejected, the adhesion of a deformed remnant film that can lubricate is probably the factor that primarily governs component lifetime (e.g., in a ball bearing). The pin-on-disk test is probably a more appropriate simulation for this situation than the thrust-washer test.

When indentation testing is used as a means of assessing adhesion, the following must be taken into account: (1) Brale indentations at variable loads have been found to generate delamination fractures near the interface between soft MoS_2 films and 440C steel. (2) A zone 2 morphology appears to have a better fracture toughness than a zone 1 morphology. (3) Substrate bombardment before deposition appears to inhibit fracture. (4) The relationship between observed fracture toughness during indentation and film adhesion during sliding contact needs to be investigated.

REFERENCES

1. M. N. Gardos, Lubr. Eng. **32**, 463 (1976).
2. R. I. Cristy, Thin Solid Films **73**, 299 (1980).
3. B. C. Stupp, Thin Solid Films **84**, 257 (1981).
4. P. Niederhauser, H. E. Hintermann, and M. Maillat, Thin Solid Films **108**, 209 (1983).
5. B. C. Stupp, Proc. 3rd Int. Conf. on Solid Lubrication, Denver, Colo., American Society of Lubrication Engineers, Park Ridge, Ill., SP-14 (1984), p. 217.
6. T. Spalvins, ASLE Trans. **14**, 267 (1971).
7. T. Spalvins, ASLE Trans. **17**, 1 (1973).
8. M. Nishimura, M. Nosaka, M. Suzuki, and Y. Miyakawa, Proc. 2nd ASLE Int. Sol. Lubr. Conf., Denver, Colo., American Society of Lubrication Engineers, Park Ridge, Ill., SP-6 (1978), p. 128.
9. T. Spalvins, Thin Solid Films **73**, 291 (1980).
10. T. Spalvins, Thin Solid Films **96**, 17 (1982).
11. V. Buck, Wear **91**, 281 (1983).
12. P. D. Fleischauer, ASLE Trans. **27**, 82 (1984).
13. T. Spalvins, Proc. 3rd Int. Conf. on Solid Lubrication, Denver, Colo., American Society of Lubrication Engineers, Park Ridge, Ill., SP-14 (1984), p. 201.
14. R. Bichsel, P. Buffat, and F. Levy, J. Phys. D: Appl. Phys. **19**, 1575 (1986).
15. V. Buck, Thin Solid Films **139**, 157 (1986).
16. V. Buck, Vacuum **36**, 89 (1986).
17. E. W. Roberts, 20th American Mechanisms Symp., NASA Lewis Research Center, Cleveland, Oh. (May 1986), p. 103.
18. E. W. Roberts, Proc. Inst. Mech. Eng., Tribology - Friction, Lubrication and Wear, Fifty Years On, London, England, Vol. I (July 1987).

19. N. J. Mikkelsen, J. Chevallier, and G. Sorensen, Appl. Phys. Lett. **52**, 1130 (1988).
20. J. R. Lince and P. D. Fleischauer, J. Mater. Res. **2(6)**, 827 (1987).
21. P. D. Fleischauer and R. Bauer, Tribology Transactions **31**, 239 (1988).
22. C. Müller, Menoud, M. Maillat, and H. E. Hintermann, Surface Coatings and Technol. **36**, 351 (1988).
23. M. R. Hilton and P. D. Fleischauer, Mat. Res. Soc. Symp. Proc. **140**, 227 (1989).
24. J. A. Thornton, Ann. Rev. Mater. Sci. **7**, 239 (1977).
25. J. A. Thornton, J. Vac. Sci. & Technol. A **4(6)**, 3059 (1986).
26. B. A. Movchan and A. V. Demchishin, Phys. Met. Metallogr. **28**, 83 (1969).
27. M. R. Hilton and P. D. Fleischauer, J. Mater. Res. **5(2)**, 406 (1990).
28. J. E. Sundgren, B.-O. Johansson, S.-E. Karlsson, and H. T. G. Hentzell, Thin Solid Films **105** (1983)
29. M. R. Hilton and P. D. Fleischauer, Thin Solid Films **172**, L81 (1989).
30. P. C. Jindal, D. T. Quinto, and G. J. Wolfe, Thin Solid Films **154**, 361 (1987).
31. J. R. Lince, J. Mat. Res **5(1)**, 218 (1990).
32. P. D. Fleischauer, Thin Solid Films **154**, 309 (1987).
33. P. D. Fleischauer, J. R. Lince, P. A. Bertrand, and R. Bauer, Langmuir **5** 1387 (1989).
34. R. L. Loh, C. Rossington, and A. G. Evans, J. Am. Ceram. Soc. **69**, 139 (1986).
35. C. Rossington, D. B. Marshall, A. G. Evans, and B. T. Khuri-Yakub, J. Appl. Phys. **56**, 2639 (1984).
36. P. K. Mehrotra and D. T. Quinto, J. Vac. Sci. Technol. A **3**, 2401 (1985).
37. S. S. Chiang, D. B. Marshall, and A. G. Evans, in J. Pask and A. G. Evans (eds.), Surfaces and Interfaces in Ceramic and Ceramic-Metal Systems, Plenum, New York, 1981, p. 603.

38. D. B. Marshall and A. G. Evans, J. Appl. Phys. **56**, 2632 (1984).
39. D. S. Rickerby, Surface Coatings and Technol. **36**, 541 (1988).

LABORATORY OPERATIONS

The Aerospace Corporation functions as an "architect-engineer" for national security projects, specializing in advanced military space systems. Providing research support, the corporation's Laboratory Operations conducts experimental and theoretical investigations that focus on the application of scientific and technical advances to such systems. Vital to the success of these investigations is the technical staff's wide-ranging expertise and its ability to stay current with new developments. This expertise is enhanced by a research program aimed at dealing with the many problems associated with rapidly evolving space systems. Contributing their capabilities to the research effort are these individual laboratories:

Aerophysics Laboratory: Launch vehicle and reentry fluid mechanics, heat transfer and flight dynamics; chemical and electric propulsion, propellant chemistry, chemical dynamics, environmental chemistry, trace detection; spacecraft structural mechanics, contamination, thermal and structural control; high temperature thermomechanics, gas kinetics and radiation; cw and pulsed chemical and excimer laser development, including chemical kinetics, spectroscopy, optical resonators, beam control, atmospheric propagation, laser effects and countermeasures.

Chemistry and Physics Laboratory: Atmospheric chemical reactions, atmospheric optics, light scattering, state-specific chemical reactions and radiative signatures of missile plumes, sensor out-of-field-of-view rejection, applied laser spectroscopy, laser chemistry, laser optoelectronics, solar cell physics, battery electrochemistry, space vacuum and radiation effects on materials, lubrication and surface phenomena, thermionic emission, photosensitive materials and detectors, atomic frequency standards, and environmental chemistry.

Electronics Research Laboratory: Microelectronics, solid-state device physics, compound semiconductors, radiation hardening; electro-optics, quantum electronics, solid-state lasers, optical propagation and communications; microwave semiconductor devices, microwave/millimeter wave measurements, diagnostics and radiometry, microwave/millimeter wave thermionic devices; atomic time and frequency standards, antennas, rf systems, electromagnetic propagation phenomena, space communication systems.

Materials Sciences Laboratory: Development of new materials: metals, alloys, ceramics, polymers and their composites, and new forms of carbon; nondestructive evaluation, component failure analysis and reliability; fracture mechanics and stress corrosion; analysis and evaluation of materials at cryogenic and elevated temperatures as well as in space and enemy-induced environments.

Space Sciences Laboratory: Magnetospheric, auroral and cosmic ray physics, wave-particle interactions, magnetospheric plasma waves; atmospheric and ionospheric physics, density and composition of the upper atmosphere, remote sensing using atmospheric radiation; solar physics, infrared astronomy, infrared signature analysis; effects of solar activity, magnetic storms and nuclear explosions on the earth's atmosphere, ionosphere and magnetosphere; effects of electromagnetic and particulate radiations on space systems; space instrumentation.